Original Article

Cytogenetic and Genome Research

Cytogenet Genome Res 2009;124:158–169
DOI: 10.1159/000207524

Accepted after revision: December 8, 2008
by M. Schmid

Studies on the short range spreading of the male specific lethal (MSL) complex on the X chromosome in *Drosophila*

X. Sun J.A. Birchler

Division of Biological Sciences, University of Missouri, Columbia, MO (USA)

Abstract

A series of autosomal insertions of chromosomal fragments derived from around the X linked white eye color locus have been examined for male specific lethal (MSL) complex binding using both immunostaining and fluorescence in situ hybridization (FISH) techniques. The results show that the transposing elements (TEs) composed of several genes in the white region (3C2-3C5) do not recruit the MSL complex when inserted into an autosome. The same result is found for the Tp(1:3)wzh insertion, a fragment of the X chromosome inserted into the third chromosome. Two other insertions, Dp(1:2)w70h (3A7-3C2-3) and Dp(1:2)51b (3C2-3D6), which extend more distally or proximally beyond the TE insertion, respectively, display a binding pattern of the MSL complex at the autosomal location. These insertions were also examined in females ectopically expressing MSL-2 and show similar binding activity. In addition, the Tp(3:1)O5 transposition strain containing an autosomal segment in the X chromosome was examined for spreading of the MSL complex. Limited spreading of the MSL complex into autosomal regions was indicated by immunostaining and FISH. This spreading was further confirmed by chromatin immunoprecipitation of the MSL complex covering the autosomal sequences.

This work was supported by NIH grant R01 JM068042.

The male specific lethal (MSL) complex consists of at least six proteins (MSL-1–3, MOF, MLE, JIL1) and two non-coding RNAs (Kelley and Kuroda, 1995; Meller et al., 1997). In males the complex binds to many sites on the X chromosome (Baker et al., 1994; Kelley et al., 1999; Demakova et al., 2003). Its presence on the male X chromosome has been hypothesized to bring about dosage compensation (Kuroda et al., 1991), but other evidence suggests a role in modifying the impact of chromosomal imbalance on genomic gene expression (Hiebert and Birchler, 1994; Bhadra et al., 1999; Pal Bhadra et al., 2005). In females the MSL complex is not formed due to the translational repression of the *msl-2* mRNA by the Sex-lethal protein (SXL) (Bashaw and Baker, 1997; Kelley et al., 1997). Ectopic expression of MSL-2 in females results in binding to the two X chromosomes (Kelley et al., 1995). MSL-1 and MSL-2 are core components of the complex, and both are required for the binding of the complex to the X (Lyman et al., 1997). The expression levels of the MSL complex are critical for its correct targeting to the X chromosome (Demakova et al., 2003). The concept that the MSL complex could spread from nucleation sites was initially proposed from two types of evidence (Bhadra et al., 1999; Kelley et al., 1999). Low level of MSL-2 in transgenic females results in a reduced number of binding sites (Kelley et al., 1997), while overexpression of MSL-2 in males extends the MSL complex spreading from *roX* transgenes into flanking autosomal

KARGER

Fax +41 61 306 12 34
E-Mail karger@karger.ch
www.karger.com

1424–8581/09/1242–0158$26.00/0

Accessible online at:
www.karger.com/cgr

James A. Birchler
Tucker Hall, University of Missouri
Columbia, MO 65211 (USA)
telephone: +1 573 882 4905; fax: +1 573 882 0123
e-mail: BirchlerJ@Missouri.edu

chromatin (Park et al., 2002). The *msl* mutations are also known to eliminate chromosomal binding of the complex to the X chromosome (Kelley et al., 1997; Lyman et al., 1997).

The mechanism of how the MSL complex recognizes its targets is unknown. The 'chromatin entry sites' model suggests that the MSL complex initially assembles at ~35 chromatin entry sites and subsequently spreads bi-directionally along the chromosome (Kelley et al., 1999). This model was proposed based on the observation that a limited number of binding sites (~35) were detected in male mutants for *mle, msl-3,* or *mof* (Kelley et al., 1997; Lyman et al., 1997). Among those high affinity sites, two have been identified and correspond to the *roX1* and *roX2* genes. Autosomal *roX* transgenes recruit the MSL complex from which it then spreads into flanking regions (Oh et al., 2003). Further studies revealed that the consensus binding region in both *roX1* and *roX2* is within male-specific DNaseI hypersensitive sites (DHS) and is represented by the two core sequences GAGAG and CTCTC (Kageyama et al., 2001; Park et al., 2003). The DHS were later found not to be required for initiation of *cis*-spreading of the MSL complex, and the *roX* RNA plays an important role in spreading (Bai et al., 2004). Further studies using ChIP-chip and ChIP-seq have extended the number of chromatin entry sites to potentially 150 or more (Alekseyenko et al., 2008). The 'entry site' model was deemed an oversimplification by further studies on chromosome transpositions, which showed that any substantial portion of the X chromosome displays a normal binding when inserted into an autosome, regardless of the presence of a previously defined entry site (Fagegaltier and Baker, 2004). This model implies that binding activity of the MSL complex to the X is dependent on the affinity of the complex to target sites and there is no spreading of the complex. This model was further tested in studies using chromatin immunoprecipitation (ChIP) (Dahlsveen et al., 2006), and the common elements for complex recruitment were analyzed.

In the present study, MSL spreading was evaluated using transposed fragments on both the X chromosome and autosomes by monitoring MSL complex recruitment and spreading. A series of autosomal insertions of X segments derived from around the *white* locus were examined for their ability to bind the MSL complex. Immunostaining followed by fluorescence in situ hybridization (FISH) revealed that not all X to A (autosome) transposition fragments accumulate the MSL complex at insertion sites but larger sections of the X will attract the complex that extends over sequences in the smaller insertions that alone have no MSL complex. In addition, by examining MSL binding in Tp(3:1)O5 flies, a transposition strain containing an autosomal segment present in the X, a limited spreading of the MSL complex at the junction into the autosomal sequences was found. Chromatin immunoprecipitation was used to confirm the nature of MSL complex spreading to the autosome segment. The results suggest that spreading of the complex does indeed occur but is limited under these circumstances.

Materials and methods

Fly strains and genetic crosses

Flies were cultured on cornmeal dextrose medium at 25°C. All the transposition stocks were obtained from the Bloomington Drosophila Stock Center (Indiana University). Their genotypes are: *y w– rst–/y+Y*; *TE89/TE89*; *z[1] w[11E4]/Dp(1:Y)y[+]*; *Tp(1:2) TE34C, kuz[3]/CyO*; *Tp(1:3)w[zh], sc[1] z[1] w[zh]*; *In(2LR)DTD86, Dp(1:2)w^{70h} ho2/In(2LR)O, Cy dp[lvl] pr cn2*; *Df(1)N-71h/C(1)M3, y[2]*; *Dp(1:2)^{51b}*/+; and *Tp(3:1)O5; D^{1}*/+ and *C(1)DX, y^{1} f^{1}*; +/+. The breakpoints of the X–autosome transpositions are listed in Fig. 1. To produce females with ectopic expression of MSL-2, a transgene [*(w^{+})H83M2–6I*] of a P-element *msl-2* construct with a *mini-white* reporter gene (Kelley et al., 1995) was introduced by crossing heterozygous males of *w–/Y*; *(w^{+})H83M2–6I/TM3* GFP with females of the transposition line. For *ISWI* mutant analysis, genetic crosses for generating the *ISWI* mutant with a TE89 insertion are diagrammed in supplementary figure 1 (online suppl. fig. 1; for suppl. material see www.karger.com/doi/10.1159/000207524). Non-GFP third instar male larvae were selected for immunostaining.

Immunostaining of chromosomes

Polytene chromosomes from the third instar larvae were dissected, fixed, and processed for antibody staining according to the protocols as described (Kuroda et al., 1991; Bhadra et al., 1999). In brief, salivary glands were dissected in 0.7% NaCl and fixed in phosphate-buffered saline (PBS) (136 mM NaCl, 1.1 mM K_2HPO_4, 2.7 mM KCl, 8.0 mM Na_2HPO_4, pH 7.3) solution containing 0.1% Triton X-100 and 3.7% formaldehyde on a siliconized coverslip for 1 min and then in 50% acetic acid, 3.7% formaldehyde for 2–5 min. The coverslip was picked up with the slide and inverted. The glands were squashed and the slides were placed in liquid nitrogen or on dry ice for the separation of the coverslip from the slide. After the removal of all coverslips, the slides were washed in PBS and blocked with PBT (PBS, 1% BSA, 0.2% Triton X-100, 0.02% azide) for 30 min. The primary antibody binding was performed at an appropriate dilution in PBT at 4°C overnight. The secondary antibody binding conjugated with fluorophore (diluted 1:100 to 1:200 in PBT) was performed at room temperature for 30 min to 3 h. The slides were mounted with Vectashield mounting medium containing 4′,6-diamidino-2-phenylindole (DAPI) (Vector Laboratory, Inc. Burlingame, CA) and examined with a Zeiss fluorescence microscope (Carl Zeiss, Inc, Oberkochen, Germany). The images were prepared using Adobe Photoshop 7.0 software.

Immunofluorescence in situ hybridization of polytene chromosomes

Probe preparation. All probes were prepared from PCR products fluorochrome-labeled by nick translation with TexasRed CTP (red) (Perkin Elmer) or AlexaFluor488-dUTP (green) (Invitrogen). Nick translation was performed according to a protocol modified from Wiegant et al. (1996). In brief, a 50 μl mixture of DNA (5 μg) with non-labeled dNTPs (0.2 mM), TexasRed CTP or AlexaFluor488-dUTP (0.05 mM), DNA polymerase I (4 U/μl), and DNase (2 mU/μl) was incubated for 2 h at 15°C. After nick translation, the probes were purified with 1× TE saturated Bio-Gel P-60 (Bio-Rad Laboratories) and ethanol-precipitated using 50 μg autoclaved salmon sperm DNA as carrier. The final pellet was dissolved in 25 μl of 1× TE, 2× SSC buffer (pH 7.0) for FISH.

Immuno-FISH. FISH was performed immediately after the second washing of slides labeled with the secondary antibody for immunostaining. Slides were fixed in 10% formaldehyde for 10 min and sequentially washed in PBS and 100% ethanol. After slides were dried, 7 μl of 1× TE, 2× SSC with 140 ng/ml of autoclaved salmon sperm DNA (Sigma) were applied to the slides at the center of the chromosome spreads. After the application of a mineral oil-coated plastic coverslip, the slides, together with the probes, were heated in a metal tray at 100°C for 5 min for denaturation. After cooling on ice, 7 μl of the probes (diluted to 20% of original) were applied to the slides for hybridization at 55°C overnight in a humidity chamber. After hybridization, slides were washed in 2× SSC for 20 min at 55°C and then mounted with Vectashield mounting medium containing DAPI as a counterstain.

Chromatin immunoprecipitation (ChIP)

Chromatin samples were prepared from third instar larvae of either males or females as described (www.igh.cnrs.fr/equip/cavalli/link.labgoodies.html; Chua et al., 2001). Briefly, 150–200 mg of third instar larvae (sufficient for four independent immunoprecipitations) was homogenized in 1.8% formaldehyde of B1 buffer (60 mM KCl, 15 mM NaCl, 4 mM $MgCl_2$, 15 mM HEPES (pH 7.6), 0.5% Triton X-100, 0.5 mM DTT, 10 mM sodium butyrate, EDTA-free protease inhibitor cocktail (Roche)) for 15 min (total time starting from beginning of homogenization) at room temperature (RT). Glycine was added to a final concentration of 225 mM and the homogenate was mixed and incubated for 5 min at RT, followed by centrifugation at 4000 *g* at 4°C with discard of the supernatant. The pellet was washed three times in B1 buffer, and once in lysis buffer (140 mM NaCl, 15 mM HEPES pH 7.6, 1 mM EDTA, 0.5 mM EGTA, 1% Triton X-100, 0.5 mM DTT, 0.1% sodium deoxycholate, 0.05% SDS, 10 mM sodium butyrate, with protease inhibitors). The same conditions applied for pelleting following each wash. The pellet was resuspended in 0.5 ml lysis buffer with addition of SDS and N-lauroylsarcosine to 0.5% each. The resuspended cross-linked material was incubated for 10 min at 4°C in a rotating wheel and then subjected to sonication. Each sample was sonicated 5–6 times for 30 s each, using a Fisher Scientific Sonicator (Model w375, Heat Systems-ultrasonic, Inc.) at output 3 and duty cycle 30%. The sonicated chromatin solution was centrifuged 5 min at RT at maximum speed to remove the debris. The supernatant was purified and concentrated with a Centricon YM-100 column (4212), pre-blocked by BSA (1 mg/ml), and centrifuged at 1000 *g* three times for 40 min while adding ChIP dilution buffer (0.01% SDS, 1.1% Triton X-100, 1.2 mM EDTA, 0.6 mM EGTA, 16.7 mM Tris-HCl, pH 8.1, 167 mM NaCl, 10 mM sodium butyrate, 0.5 mM DTT, with protease inhibitors). 100 μl protein G agarose/salmon sperm DNA beads (Upstate Scientific Technology) equilibrated with ChIP buffer was added to samples for pre-clearance at 4°C on a rotation wheel for 4 h. Immunoprecipitation (IP) was then performed on a sample of the supernatant collected from pre-incubation using 3 μl/IP of MSL-2 polyclonal antibody (Santa Cruz) incubated overnight at 4°C, using no antibody as a control. After antibody binding, 60 μl of protein G agarose beads were added and incubated on a rotating wheel at 4°C for 4 h. Beads were then subsequently washed with a low salt buffer (0.1% SDS, 1% Triton X-100, 2 mM EDTA, 20 mM Tris-HCl, pH 8.1, 150 mM NaCl), a high salt buffer (0.1% SDS, 1% Triton X-100, 2 mM EDTA, 20 mM Tris-HCl, pH 8.1, 500 mM NaCl), a lithium chloride wash buffer (0.25 M LiCl, 1% IGEPAL CA630, 1% deoxycholic acid (sodium salt), 1 mM EDTA, 0.5 mM EGTA, 10 mM Tris, pH 8.1, 10 mM sodium butyrate, 0.5 mM DTT), and then two washes of TE (10 mM Tris-HCl, 1 mM EDTA, pH 8.0). The immunoprecipitated protein/DNA was eluted in 500 μl elution buffer (1% SDS, 0.1 M $NaHCO_3$) at 65°C for 15 min. Beads were removed and then the samples were reverse cross-linked, with addition of 25 μl of 4 M NaCl, and 5 μl of Proteinase K (10 mg/ml), and incubated at 65° for 5 h. Following reversal of cross-links, the precipitated DNA was recovered using phenol/chloroform extraction and ethanol precipitation, and then re-suspended in 20 μl of nuclease-free H_2O. 1 μl of this DNA was used as a template for real-time PCR.

Relative quantification of DNA fragments from ChIP by real-time PCR

Real-time PCR was performed on the resuspended DNA from ChIP described above using the Power SYBR Green PCR Master Mix kit (ABI). Three sets of primers were chosen. Two pairs (5′-88B and 92C-3′) were designed for cytologically visualized binding regions adjacent to each breakpoint, and one pair (88B-150K) was designed for a non-binding region as an internal control. The primer sequences were as follows: for 5′-88B: 5′-ACT TGT TGT GAA TTG TGC CGT GGG-3′ (forward) and 5′-TCA AGC CAT CAT GTT GAA GTG GCG-3′ (reverse), for 92C-3′: 5′-TCC ACC CTC AAT CTT GGA GGA ACA-3′ (forward) and 5′-TTT GGG ACA TGG GCT TGG GTT T-3′ (reverse), and for 88B-150K: 5′-GGC TGG GTG CAG CGA AAT GAA TAA-3′ (forward) and 5′-TGC CTC GCC AAT TGA GTT TAT GCC-3′ (reverse). PCR amplification and fluorescence detection were performed in a 25 μl final volume containing 100 ng of each primer and 1 μl of the immunoprecipitated DNA using the Applied Biosystems 7300 Real-Time PCR System with a thermocycler profile of 50°C for 2 min, 95°C for 10 min, and followed by 40 cycles of 95°C for 15 s, 55°C for 1 min. Each sample was processed three times. Primers for *β-tubulin* (forward: 5′-AGC TCA GCA CCC TCT GTG TAA T-3′ and reverse: 5′-AGC TGG AGC GCA TCA ATG TGT A-3′) were used as the internal reference for normalizing the amount of immunoprecipitated DNA on the basis of the different Ct value. The relative quantification (RQ) for each primer was determined according to the ΔCt analysis based on the manufacturer's instructions (Applied Biosystems 7300 Real-Time PCR system, sequence detection software Version1. 3.1.).

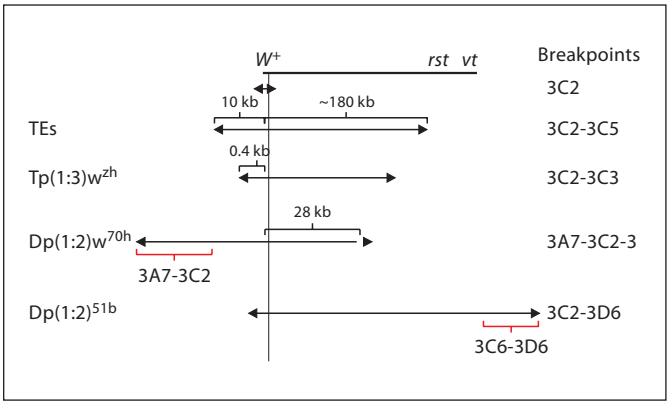

Fig. 1. A diagram of insertions showing their lengths and cytological breakpoints. All the lines have an autosomal insertion of an X chromosome fragment surrounding the *w* gene (3C2). The detailed genotype for each insertion is described in Materials and methods and Flybase (www.flybase.org). The *roughest (rst)* and *vertical (vt)* genes are proximal to *w*, at 3C3-3C4 and 3C5+, respectively. The *rst* and *vt* sequences are not detected in the transposed fragment of Tp(1:3)w^{zh} (see Fig. 4). The difference between Dp(1:2)w^{70h} and the TEs distal breakpoints and between Dp(1:2)^{51b} and the TEs proximal breakpoints are shown in red.

Results

MSL complex binding to X chromosome derived fragments inserted into an autosome

Previous studies had suggested that very small X chromosome derived fragments could not attract the MSL complex at autosomal positions, which were, however, bound by the complex if present in a larger context on the X chromosome or in a larger X–autosomal transposition (Bhadra et al., 1999). This finding led to the proposal that the MSL complex could spread from nucleation sites (Bhadra et al., 1999). Indeed, extensive spreading was subsequently found from transgenes carrying the *roX* genes (Kelley et al., 1999), confirming the concept of spreading. To examine this issue further, the MSL complex binding was first examined in various autosomal insertions of X fragments. The fragments tested were all derived from around the *w* gene and were of differing lengths, including the transposing elements (TEs) and transpositions depicted in Fig. 1. The *w* locus is located in the 3C2 region of the salivary gland polytene map and is about 5.9 kb in length. The TEs tested in this study included TE89 and Tp(1:2)TE34C, both having the smallest piece of X chromosome examined in this study (3C2-3C5). An independent small insertion examined was Tp(1:3)w^{zh} (3C2-3C3). Another insertion, Dp(1:2)^{51b}, was reported to extend more proximally on the X than the TEs, with breakpoints of 3C2-3D6 (www.flybase.org). Another insertion, Dp(1:2)w^{70h} (3A7-3C2-3), has a proximal breakpoint within the TE limits but extends much more distally. From immunostaining and FISH studies in normal males, the TEs are not labeled at all with anti-MSL-2 antibodies, which indicates that no MSL complex is recruited to them (Fig. 2). Similarly, there is no complex binding observed for the Tp(1:3)w^{zh} insertion (Fig. 2C). Two larger insertions, Dp(1:2)w^{70h} and Dp(1:2)^{51b}, were found to attract the MSL complex (Fig. 2D, E), and a similar recruitment was also found in females with ectopic expression of MSL-2, generated by crossing the *msl-2* transgene *(w+)H83M2–6I* into these transposition lines (Fig. 2F, G). This result indicates that if the X–autosome transposition can recruit the MSL complex in normal males, the inserted piece of X chromosome is also sufficient to recruit the MSL complex in females with ectopic expression of MSL-2.

The *ISWI* mutation causes a bloated chromosome phenotype that is much stronger for the X chromosome in the presence of the MSL complex (Corona et al., 2002). The related mutation, *nurf310*, causes a similar effect that can be visualized for a single transgene (Badenhorst et al., 2002; Bai et al., 2007). To test further if the TE segment associates with the MSL complex, binding was examined in the *ISWI* mutant together with TE89. The TE89 was crossed into *ISWI* mutant lines, and the polytene chromosomes were probed with anti-MSL-2 antibodies. As indicated in Fig. 3, the TE insertion, in the *ISWI* mutant background, does not change in morphology to produce a comparable bloated site in the autosome relative to the location on the normal X (Fig. 3).

It is interesting that the TEs and Tp(1:3)w^{zh} do not recruit the MSL complex to their autosomal insertion sites, while the two larger duplications show the MSL complex colocalizing with the *white* FISH signal. Comparing one of the duplications Dp(1:2)^{51b} to the Tp(1:3)w^{zh} insertion, it can be hypothesized that a nucleation site for MSL binding exists between the proximal breakpoints of the Tp(1:3)w^{zh} and the Dp(1:2)^{51b} duplication (Fig. 1). Similarly, the sequence between the distal breakpoints of the TEs and Dp(1:2)w^{70h} (Fig. 1) might contain another nucleation site.

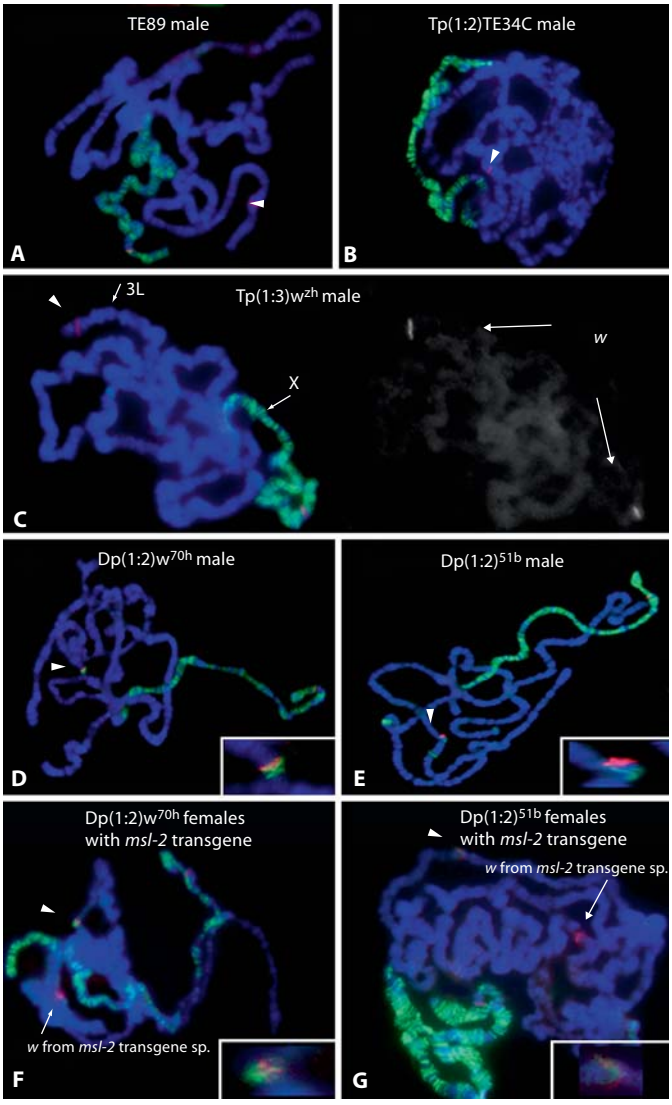

Fig. 2. MSL binding to X chromosomal fragments inserted into autosomes. Polytene chromosomes from third instar larvae of each transposition were fixed, squashed, and labeled with anti-MSL-2, followed by fluorescence in situ hybridization (FISH) using the *w* gene as a probe. DNA stain (DAPI) is in blue, anti-MSL-2 staining in green, and the *w* FISH probe in red. The primer sequences for the *w* probe are 5′-GGA ACC ACT CAC CGT TGT CT-3′ (forward) and 5′-TAT TCT GCA ACG AGC GAC AC-3′ (reverse), amplifying exon 1 of *w*. A merged image is presented for each insertion line. In addition, the gray value FISH channel was included for the Tp(1:3)w^{zh} male (**C**), showing the *w* gene from the autosomal insertion and on the X chromosome. The lines showing the MSL binding on autosomal insertions (**D**, **E**) were also immunostained in females expressing ectopic MSL-2 (**F**, **G**). The insertion region showing the MSL binding is magnified at the lower right insets. Both duplications, Dp(1:2)w^{70h} and Dp(1:2)^{51b}, were able to recruit the MSL complex, whether in males or in females with ectopic expression of MSL-2 in contrast to the TEs (**A**, **B**) or Tp(1:3)w^{zh}(**C**). The images of females with ectopic expression of MSL-2 are in the bottom panels showing an extra *w* gene signal arising from the *msl-2* transgene carrying a *mini-white* as a reporter gene. The arrowhead in each image indicates the inserted segment on the respective autosome.

Cytologically, the genes *roughest (rst)* and *verticals (vt)* are located proximal to the *w* gene. In situ hybridization to polytene chromosomes of wild type shows that those genes are close together in the 3C region (Fig. 4A–D). The transposed insertions TE89, Tp(1:3)w^{zh} and Dp(1:2)^{51b}, overlapping at their distal ends (see Fig. 1), were examined for the presence of the *rst* (3C3-3C4) and/or *vt* (3C5+) genes. The results show that both *rst* and *vt* were observed in Dp(1:2)^{51b} (Fig. 4I–L), but not in the Tp(1:3)w^{zh} insertion (Fig. 4E–H). The *rst* gene was also contained in the TE89 insertion (Fig. 4M–P). Thus, the Tp(1:3)w^{zh} insertion contains less X chromosomal material than the TEs. Because the MSL complex covers the extent of the larger insert, which contains the sequences of the smaller ones, this result suggests that a site in the larger construct nucleates short range spreading, as previously suggested (Bhadra et al., 1999).

Limited MSL complex spreading to an autosomal fragment inserted into the X chromosome

Kelley et al. (1999) have found that autosomal insertion of the *roX* genes will recruit the MSL complex and that the MSL complex spreads into the adjacent autosomal regions. Another region of 18D10 on the X chromosome was also reported to have a similar binding pattern of MSL binding, when inserted into an autosome (Oh et

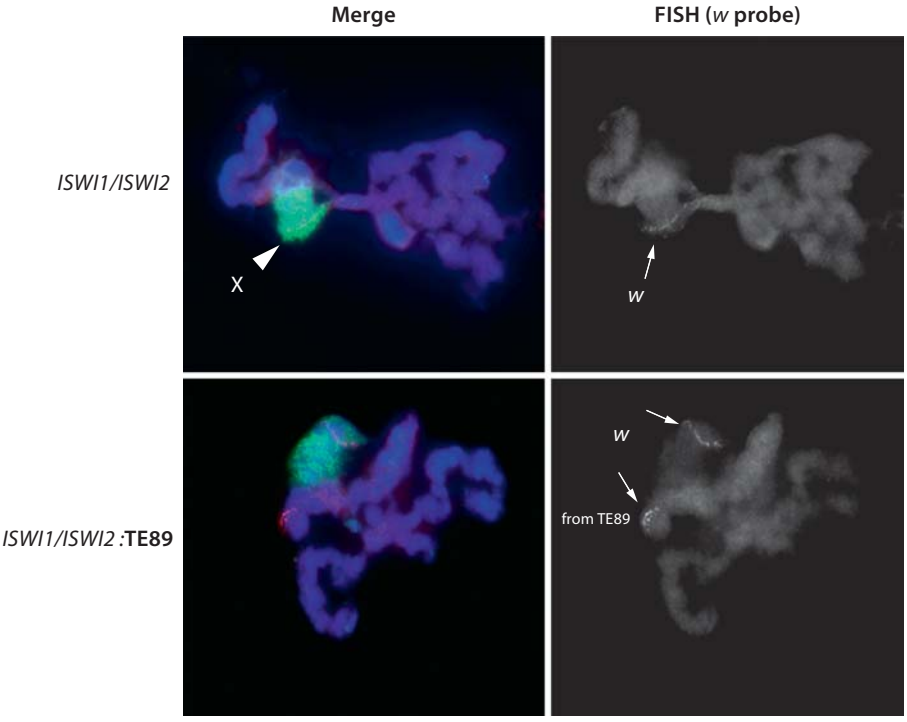

Fig. 3. MSL binding in the *ISWI* mutant with transposition of TE89. Polytene chromosomes of *ISWI* mutant males (upper panel) and *ISWI* mutants homozygous for TE89 insertion (lower panel) were probed with anti-MSL-2, followed by FISH using *w* as a probe as described in Fig. 2. Left side of each panel shows merged images, with the DNA signal in blue, anti-MSL-2 staining in green, and the *w* FISH probe in red. The right side of each panel shows the FISH signals of the *w* gene from different locations. The *ISWI* mutant shows only the endogenous *w* gene on the X chromosome. The other panel, containing the X–autosome insertion TE89, also shows the *w* gene on the autosome. There is no MSL complex observed on TE89, and *ISWI* produces no bloating effect compared to *w* on the X.

al., 2004). However, the results from Fagegaltier and Baker (2004) and Oh et al. (2004) indicate that when an autosomal fragment was inserted into the X chromosome, there was no MSL complex binding observed on the insertion, suggesting no spreading of the MSL complex in normal males. On a large scale view, this is obvious (Fig. 5). However, to test the possibility of short range spreading, the binding of the MSL complex to Tp(3:1)O5 was examined. Immunostaining for MSL-2 in Tp(3:1)O5 male flies revealed the presence of limited spreading of the MSL complex at either side of this insert as revealed by the overlap of signals from the MSL complex and autosomal sequences labeled by FISH probes (Fig. 5A–C, E, F). The FISH probes were generated from different primers designed near each breakpoint on the autosomal fragment. The primer sequences, resulting product sizes, and binding regions on the autosome are summarized in Table 1. This result suggests that the MSL complex on the X chromosome can spread onto autosomal sequences, roughly limited to 4–5 kb in distance on each side of the insertion (Fig. 6).

The accuracy of colocalization might be obscured by cytological methods and photographic exposure time. In order to confirm the spreading of the MSL complex from the X into the autosomal regions, chromatin immunoprecipitation (ChIP) was performed using anti-MSL-2, followed by real-time PCR for amplification of DNA fragments immunoprecipitated from binding regions. Three pairs of primers were used to measure the enrichment of binding sequences (Fig. 7). Two pairs were designed within autosomal binding regions observed from in vivo immunostaining, one pair from upstream of the 88B binding region (Fig. 5C), and the other pair from downstream of the 92C binding region (Fig. 5F), designated 88B-5′ and 92C-3′, respectively. The third pair (called 88B-150K) located more internally at 88B and proximally about 150 kb beyond the binding region (Fig. 5D), was used as a control sequence (no recruitment of MSL complex on polytene chromosomes). Rather than using the entire binding sequence, the size was reduced to ~220-bp fragments for immunoprecipitation detection. Females were also selected as a negative control compared to males for each pair of primers to test the enrichment of DNA sequence from immunoprecipitation, as there is no MSL-2 on the X or autosomes in females. Relative quantification of binding sequence was measured by real-time PCR. From this study, compared to the control IP, the 5′ end of 88B and the 3′ end of 92C are both enriched in the MSL-2-immunoprecipitation in males but not in females, and the internal region (88B-150K) also did not accumulate MSL-2

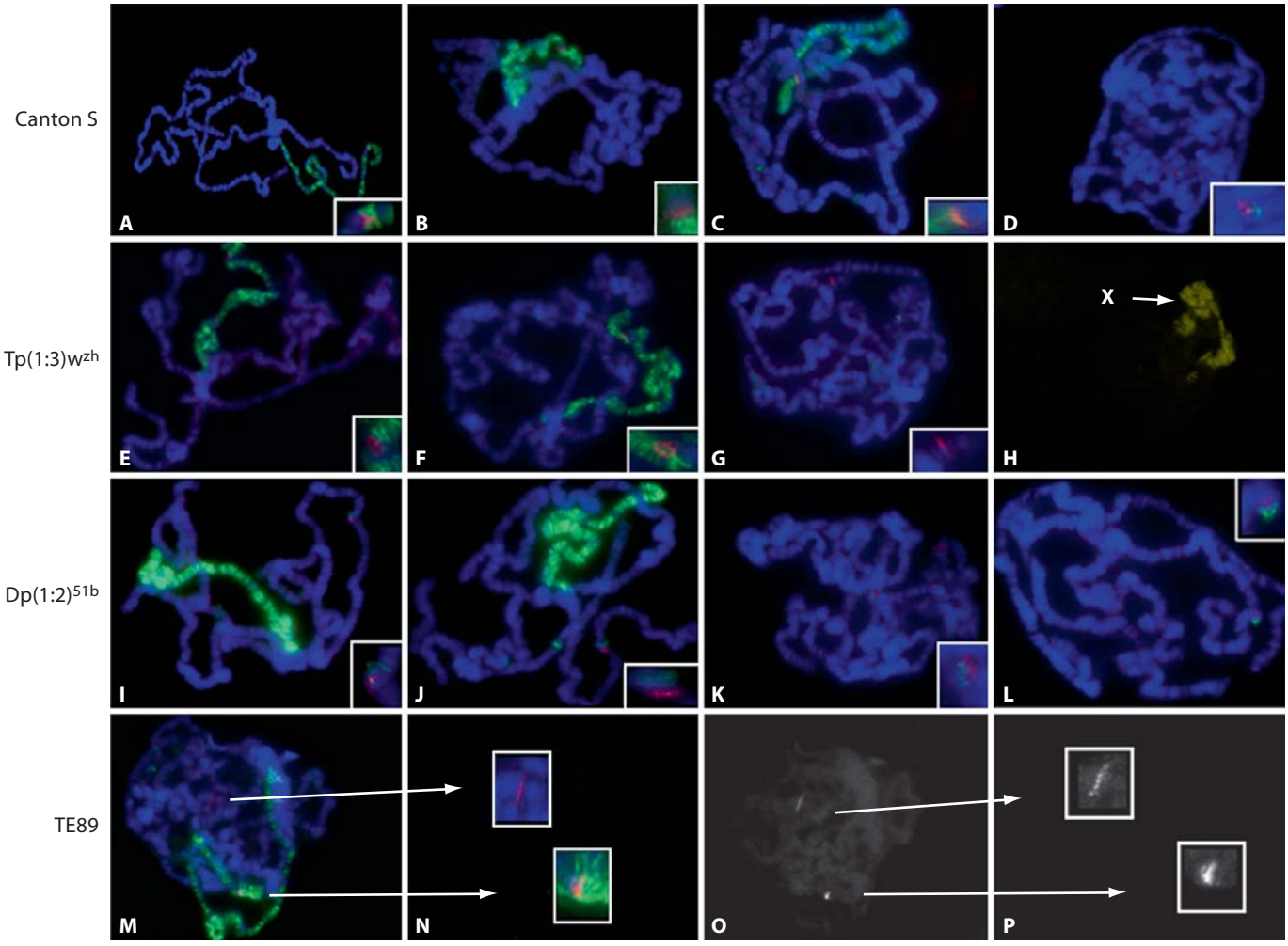

Fig. 4. Detection of *rst* and *vt* genes in autosomal insertions using FISH probes of *w, rst,* and *vt,* individually or mixed. Canton S wild type was used as a reference to define the location of *rst* and *vt*. Anti-MSL-2 staining was performed to determine if there is MSL binding surrounding *rst* or *vt*. Triple labeling with antibody and two FISH probes was used. An enlarged view for the location of *rst* and *vt* either on the X or the insertions is shown in the bottom right of each image. Locations of *rst* (**A**), *vt* (**B**), and *w* (**C**), all labeled in red on the X chromosome (labeled with MSL-2 in green) of Canton S. **D** shows the two genes *w* (red) and *vt* (green) as neighboring genes. *rst* (**E**) and *vt* (**F**) genes (red) are only located on the X (in green) of the Tp(1:3)w^{zh} line, but not on the autosomal insertion site which is verified by the *w* gene probe (red) in **G**, in which *rst* is shown in green. **H** shows the same nucleus as in **G** with the channel showing the X chromosome location to confirm that the *vt* gene shown in **G** is only on the X. *rst* (**I**) and *vt* (**J**) genes (red) both located on an autosome in the Dp(1:2)^{51b} line. (There is no *rst* and *vt* on the X due to the deletion of 3C4-D4 in this stock). MSL-2 binding is shown in green. Both *rst* (**K**) and *vt* (**L**) (green) are localized near the *w* gene (red) on the autosomal insertion site. **M** shows that *rst* (red) is located on the autosomal insertion of the TE89 line. **N** shows the magnified signals in **M**. **O** shows *rst* signals in the red channel and magnified in **P**.

Fig. 5. MSL binding to portions of the autosome inserted into the X chromosome in Tp(3:1)O5. Polytene chromosomes from Tp(3:1)O5 males were labeled with anti-MSL-2 (green), followed by FISH using different probes (red) generated from primers listed in Table 1. Immunolabeling and FISH images are presented, showing binding regions at the borders of the insertion site. The FISH probes also hybridize to the normal chromosome 3 in each nucleus. An image showing no MSL binding was also selected for comparison. (**A**) Binding at 88A, in the region of 382.120–382.920 kb. (**B**, **C**) Binding at 88B, in the regions of 320–1093 bp (**B**) and 1.341–2.056 kb (**C**), respectively. (**D**) No binding in the region of 150.419–151.383 kb. (**E**, **F**) Binding at 92C, in the regions of 95.275–95.995 kb (**E**) and 99.154–99.869 kb (**F**), respectively. An enlarged view for the location of MSL binding is shown in each image.

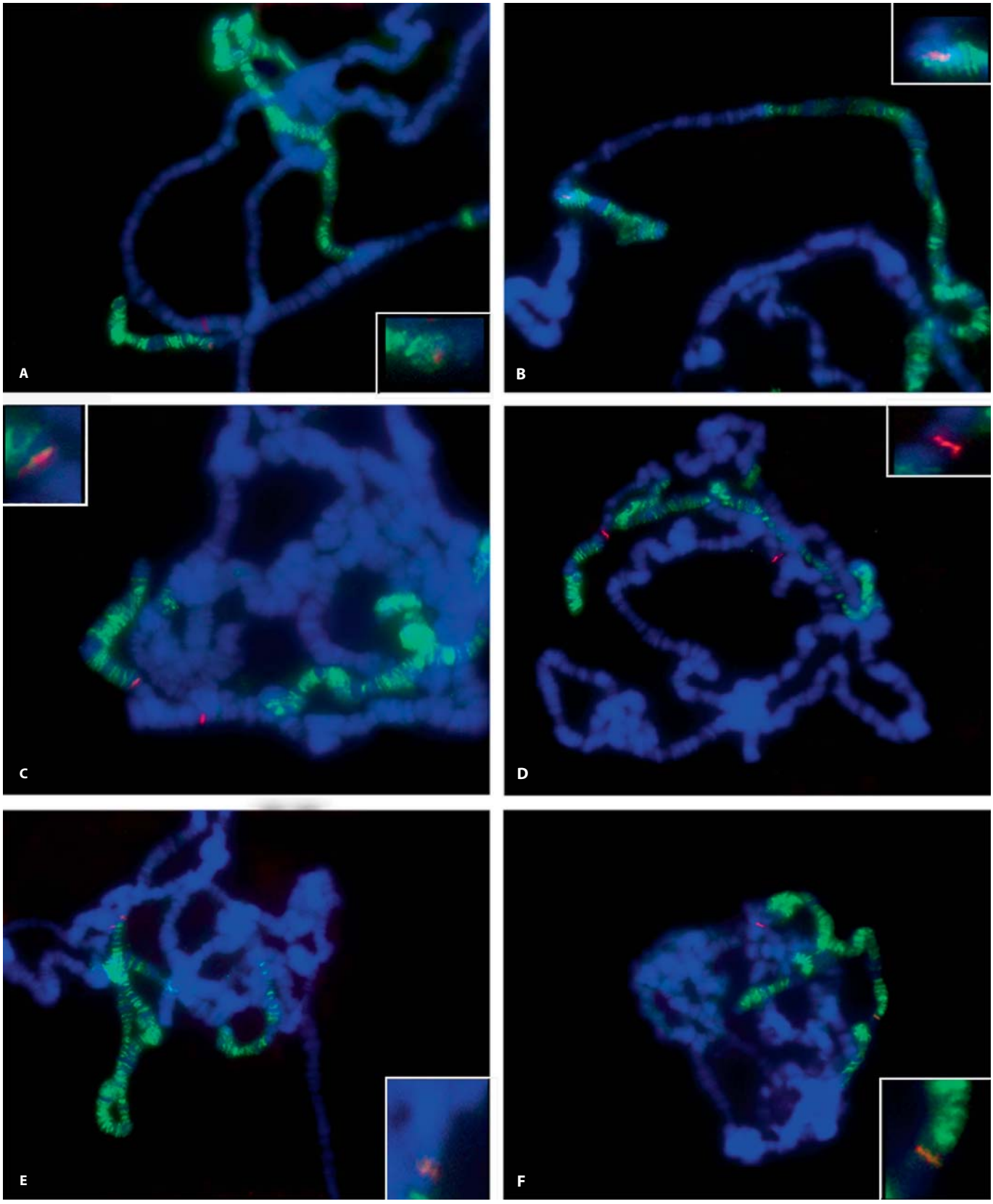

5

Table 1. Summary of MSL complex binding in the autosomal fragment inserted into the X chromosome in Tp(3:1)O5

Primer	Location	Primer sequences (5′–3′)	MSL binding
88A	300.411–301.242 kb	F: GGC AAA GTG TGT GGC CGT TTA GAT R: TCG CAT CAG TGT GAA GTG GAG TGT	–
88A	302.148–302.857 kb	F: TGG CTG CAA GTT CAC CCA ATG TAG R: CAG CAA AGG CTG CTG TCA AAG GAA	–
88A	370.212–370.981 kb	F: AAC ACC CGA TCG GAG ACA AAG ACA R: TCC AAT GAC AAA TGC AAT GCG GGC	–
88A	382.120–382.920 kb	F: TAC TGC TCC AGT ATC GCC CTC ATT R: CAA ACT TGT CCG GGC GGA ATT CAA	+
88B	11–795 bp	F: ATA CGG AAT GAG TGA GCC CAC AGT R: TGC TGT CAG GCG TAA ACT AAG CCA	+
88B	320–1093 bp	F: TTG CGA CGG TAA CAA CCA ATG CTG R: TGT CGC TAT AAA CGT CGA CCC ACA	+
88B	1.341–2.056 kb	F: ACT TGT TGT GAA TTG TGC CGT GGG R: TTA CTG GCA TTG CCT CGA ACA CCT	+
88B	5.096–5.916 kb	F: TGG GAA CCT GGA CTG GCT TAC AA R: TGA ATG TCA AGT GCA GGA CGA GGA	–
88B	50.251–50.972 kb	F: AGG CCA GAG GTT GTT GCT TCA CTA R: AAA CCC TCC AAG TCG ATC AAC CGT	–
88B	70.149–70.966 kb	F: AGC CGA GCA TGT CTG ATG TCT CAA R: TGC CTT TCA GCG GTG TTA CTT CCT	–
88B	150.419–151.383 kb	F: GCG TTC TCT TGG CTG AAT GCC TTT R: TGT GAC TGC CAT TAC CAA GGC TCT	–
88C	108–1051 bp	F: ACA AGT TGG TTG GTC TGT TTC GGG R: TCC CGT GTA ATC TCT GGT TGC CTT	–
92C	95–971 bp	F: GGG TGT GTG GTT AAG CTG CCA TTT R: GGG TGG CAA CAT AAC TAA CGG CAA	–
92C	48.518–49.447 kb	F: GAA GTT GCC TGT GCG AGA AAG CAT R: TCT ACA AGC TCA CCT TCT GGC TCT	–
92C	80.180–80.969 kb	F: TGA ACG CAG TTC AAA GCT GCT CCT R: GGC TTG TGT TCC AAA CAG CTG CAA	–
92C	95.275–95.995 kb	F: TGT GAC ACT TAG CTC AGC CAA AGC R: TCC AGT TTG AAG TTT CCC GAG CTG	+
92C	99.154–99.869 kb	F: ATT TCT GCC AAG GGT TAT GCC CAC R: TGT GGA CGC CTT TAT TGT TTG CCC	+
92C	100.015–100.927 kb	F: GGG ATG TTG TTG GCT TTG GTG TCA R: ACT TAA TAG GCC ACG CTC GCT CTT	–
92D	525–1439 bp	F: ATA TGC AGA TAA ATT CCG GGC GGC R: AGC GTA TGC GTG TTT GTG TGA GTG	–

The regions 88A–C and 92C–D are the two breakpoints on the autosomal portion of Tp(3:1)O5. Genomic size of each region is 88A: 383.096 kb, 88B: 188.671 kb, 88C: 260.715 kb, 92C: 125.636 kb, and 92D: 162.310 kb. Based on the genomic sequences (www.flybase.org), a series of sets of primers were designed using primerquest software (www.idtnda.com) in the regions 88A, 88B, 88C, 92C, and 92D. The primers span regions remaining on the autosomal segment inserted into the X chromosome. For example, 88A-300.411–301.242 kb indicates the PCR product amplified for a FISH probe that spans the region from 300.411 to 301.242 kb. The PCR products amplified from each pair of primers were identified by gel analysis and the ones with only one band were used generating probes for further studies.

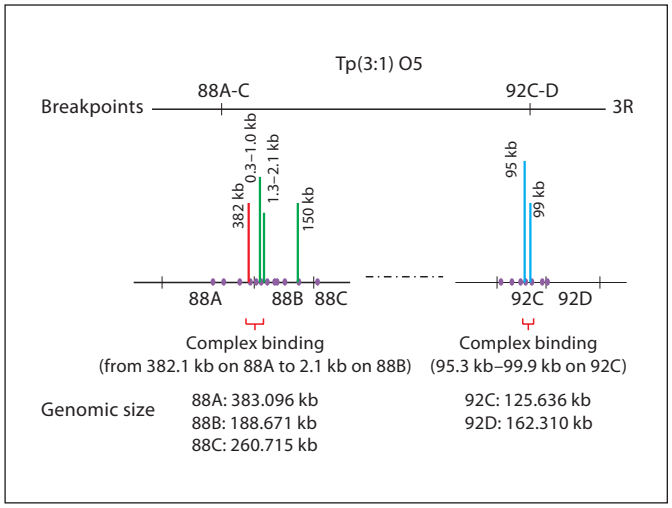

Fig. 6. A diagram showing the breakpoints and binding regions in 3R of Tp(3:1)O5. The top line represents the 3R chromosome with the two breakpoints of 88A-C and 92C-D. The bottom half of the diagram shows the specific regions screened for MSL complex binding, with a total of 19 locations indicated by purple dots (see Table 1 for detailed information on primer sequences). The colored vertical lines show the locations selected for immunolabeling and FISH image display shown in Fig. 5, including regions with and without complex binding. The putative binding regions at each breakpoint are defined.

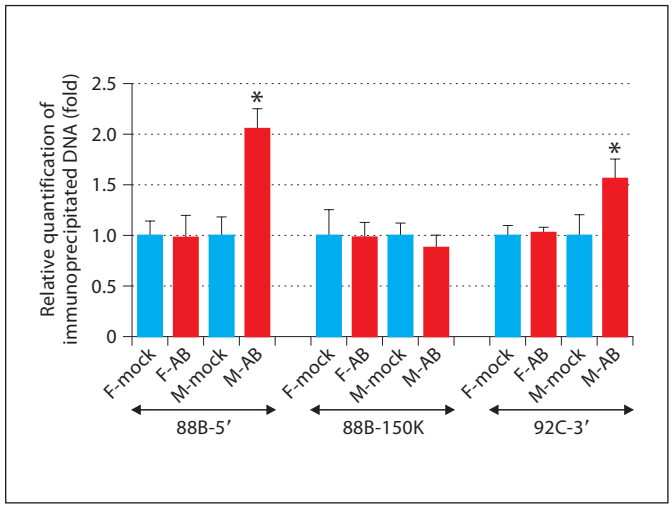

Fig. 7. Relative quantification of immunoprecipitated DNA by real-time PCR at different binding regions. The real-time PCR analysis was used to validate the in vivo observation from immunolabeling-FISH studies showing that the MSL complex spreads into autosomal sequences inserted into the X chromosome in Tp(3:1)O5 flies (Fig. 5). Three different pairs of primers, two representing binding regions and one in a non-binding region, were used for amplifying DNAs immunoprecipitated by a MSL-2 polyclonal antibody in those regions. The relative quantification was expressed as fold change in the amount of DNA enriched from anti-MSL-2 immunoprecipitated samples of males or females (red bars) of Tp(3:1)O5, compared to their respective controls (without antibody, blue bar) for a specific pair of primers. The standard errors shown on the bars are based on three biological replicates. Samples with means significantly different from the mock control at <5% confidence level are marked by an asterisk. F-mock: female control samples (without MSL-2 antibody). F-AB: female sample immunoprecipitated with MSL-2 antibody. M-mock: male control samples (without MSL-2 antibody). M-AB: male sample immunoprecipitated with MSL-2 antibody. 88B-5′: a pair of primers designed in the binding region at 88B. 92C-3′: a pair of primers designed for the binding region at 92C. 88B-150K: a pair of primers designed at a non-binding region located near 150K of 88B, used as an internal negative control.

in chromatin immunoprecipitation in either males or females (Fig. 7). The ChIP results are in concordance with the polytene immunolabeling and observations (Fig. 5), suggesting that the MSL complex on the X chromosome can spread into autosomal sequences over a short range.

Discussion

Binding targets of the MSL complex

Using immunostaining and FISH, the recruitment of the MSL complex in different transposition insertions derived from around the *w* gene have been examined. Applying FISH for *white* in this study established the exact site for assaying MSL association. The results show that transpositions of sufficient length are able to recruit the MSL complex. Examination of TE89, the larger of the nonbinding autosomal inserts, in an *ISWI* background confirmed that it does not attract the MSL complex. *ISWI* mutants show a 'bloated' chromosome phenotype, and the effect is greatly amplified by the MSL complex (Corona et al., 2002; Pal Bhadra et al., 2005). If the TEs can recruit the MSL complex to its insertion site in an autosome, it should show this chromosomal phenotypic effect to some extent similarly to the *nurf310* mutants (Bai et al., 2007).

The transposition Tp(1:3)w^{zh} males do not show binding at its insertion site of 61D (Fig. 2C). This result differs from the claims of Fagegaltier and Baker (2004), who reported the recruitment of the complex on this insertion site. However, our results were confirmed using a FISH probe of the *w* gene, a sequence contained in each insertion. By using this probe, another site of MSL binding on 3L was excluded (Fig. 2), which might account for this

discrepancy. A combination of both TE89 and Tp(1:3)w^{zh} was also examined for the binding of the MSL complex; the labeling of the MSL complex was not seen at either insertion site as verified by *w* gene FISH (not shown). Unlike TEs and Tp(1:3)w^{zh}, the two larger insertions Dp(1:2)w^{70h} and Dp(1:2)^{51b} show binding to the MSL complex in males (Fig. 2D, E). This binding ability also occurs in females with ectopic expression of MSL-2 (Fig. 2F, G), showing that the level of ectopic MSL-2 is sufficient to recruit the MSL complex. These data suggest that MSL target determinants are present in these insertion sequences and are located outside of the limits of TE or Tp(1:3)w^{zh} (Fig. 1). These regions might contain a common consensus DNA motif comparable to other DNA binding fragments (DBFs) (Dahlsveen et al., 2006; Alekseyenko et al., 2008). In this study, the single genes *rst* and *vt* were probed, and we found that *vt* is present in Dp(1:2)^{51b} (Fig. 4I–L) but not in Tp(1:3)w^{zh} (Fig. 4E–H). The *rst* gene is excluded as containing a binding target because it is present in the TE insertion (Fig. 4M–P).

Limited spreading of the MSL complex

Most strikingly, using immunolabeling and FISH analyses, we visualized the spreading of the MSL complex into autosomal sequences in Tp(3;1)O5 (Fig. 5). The spreading is limited to a few kilobases (see Table 1), which is not as extensive as observed with *roX* transgenes that condition a long range spreading up to 1 Mb (Kageyama et al., 2001). ChIP analysis was performed with an MSL-2 antibody followed by real-time PCR using autosomal primers to confirm the local spreading. Female samples and the 80B-150kb primers (located near the genomic position 150 kb of 88B) were both used as negative controls. Autosomal sequences adjacent to the X breakpoints were precipitated at much greater amounts in males indicating that there is complex spreading from the X regions. Oh et al. (2004) examined Tp(3:1)O5 using only chromosomal immunostaining and concluded that there was no spreading into autosomal sequences, which is true in a global sense. Here, the combined immunolabeling and FISH, together with the more sensitive ChIP procedure, reveals limited spreading, which would likely not be detected in the aforementioned study. The results do indicate an affinity of X fragments for the MSL complex and constraints on extensive spreading into autosomal sequences, which is consistent with the general conclusions of Fagegaltier and Baker (2004), Oh et al. (2004), Dahlsveen et al. (2006), and Alekseyenko et al. (2008) concerning MSL spreading.

References

Alekseyenko AA, Peng S, Larshan E, Gorchakov AA, Lee O-K, et al: A sequence motif within chromatin entry sites directs MSL establishment on the *Drosophila* X chromosome. Cell 134:599–609 (2008).

Badenhorst P, Voas M, Rebay I, Wu C: Biological functions of the ISWI chromatin remodeling complex NURF. Genes Dev 16:3186–3198 (2002).

Bai X, Alekseyenko AA, Kuroda MI: Sequence-specific targeting of MSL complex regulates transcription of the *roX* RNA genes. EMBO J 3:2853–2861 (2004).

Bai X, Larschan E, Kwon SY, Badenhorst P, Kuroda MI: Regional control of chromatin organization by noncoding *roX* RNAs and the NURF remodeling complex in *Drosophila melanogaster*. Genetics 176:1491–1499 (2007).

Baker BS, Gorman M, Marin I: Dosage compensation in *Drosophila*. Annu Rev Genet 28: 491–521 (1994).

Bashaw GJ, Baker BS: The regulation of the *Drosophila msl-2* gene reveals a function for *Sex-lethal* in translational control. Cell 89:789–798 (1997).

Bhadra U, Pal Bhadra M, Birchler JA: Role of the *male specific lethal (msl)* genes in modifying the effects of sex chromosomal dosage in *Drosophila*. Genetics 152:249–268 (1999).

Chua YL, Brown AP, Gray JC: Targeted histone acetylation and altered nuclease accessibility over short regions of the pea plastocyanin gene. Plant Cell 13:599–612 (2001).

Corona DF, Clapier CR, Becker PB, Tamkun JW: Modulation of ISWI function by site-specific histone acetylation. EMBO Rep 3:242–247 (2002).

Dahlsveen IK, Gilfillan GD, Shelest VI, Lamm R, Becker PB: Targeting determinants of dosage compensation in *Drosophila*. PLoS Genet 2: e5 (2006).

Demakova OV, Kotlikova IV, Gordadze PR, Alekseyenko AA, Kuroda MI, Zhimulev IF: The MSL complex levels are critical for its correct targeting to the chromosomes in *Drosophila melanogaster*. Chromosoma 112: 103–115 (2003).

Fagegaltier D, Baker BS: X chromosome sites autonomously recruit the dosage compensation complex in *Drosophila* males. PLoS Biol 2:e341 (2004).

Hiebert JC, Birchler JA: Effects of the *maleless* mutation on X and autosomal gene expression in *Drosophila melanogaster*. Genetics 136:913–926 (1994).

Kageyama Y, Mengus G, Gilfillan G, Kennedy HG, Stuckenholz C, et al: Association and spreading of the *Drosophila* dosage compensation complex from a discrete *roX1* chromatin entry site. EMBO J 20:2236–2245 (2001).

Kelley RL, Kuroda MI: Equality for X chromosomes. Science 270:1607–1610 (1995).

Kelley RL, Solovyeva I, Lyman LM, Richman R, Solovyev V, Kuroda MI: Expression of *msl-2* causes assembly of dosage compensation regulators on the X chromosomes and female lethality in *Drosophila*. Cell 81:867–877 (1995).

Kelley RL, Wang J, Bell L, Kuroda MI: *Sex lethal* controls dosage compensation in *Drosophila* by a non-splicing mechanism. Nature 387: 195–199 (1997).

Kelley RL, Meller VH, Gordadze PR, Roman G, Davis RL, Kuroda MI: Epigenetic spreading of the *Drosophila* dosage compensation complex from *roX* RNA genes into flanking chromatin. Cell 98:513–522 (1999).

Kuroda MI, Kernan MJ, Kreber R, Ganetzky B, Baker BS: The maleless protein associates with the X chromosome to regulate dosage compensation in *Drosophila*. Cell 66:935–947 (1991).

Lyman LM, Copps K, Rastelli L, Kelley RL, Kuroda MI: *Drosophila* male-specific lethal-2 protein: structure/function analysis and dependence on MSL-1 for chromosome association. Genetics 147:1743–1753 (1997).

Meller VH, Wu KH, Roman G, Kuroda MI, Davis L: *roX1* RNA paints the X chromosome of male *Drosophila* and is regulated by the dosage compensation system. Cell 88:445–457 (1997).

Oh H, Park Y, Kuroda MI: Local spreading of MSL complexes from *roX* genes on the *Drosophila* X chromosome. Genes Dev 17:1334–1339 (2003).

Oh H, Bone JR, Kuroda MI: Multiple classes of MSL binding sites target dosage compensation to the X chromosome of *Drosophila*. Curr Biol 14:481–487 (2004).

Pal Bhadra MP, Bhadra U, Kundu J, Birchler JA: Gene expression analysis of the function of the male-specific lethal complex in *Drosophila*. Genetics 169:2061–2074 (2005).

Park Y, Kelley RL, Oh H, Kuroda MI, Meller VH: Extent of chromatin spreading determined by *roX* RNA recruitment of MSL proteins. Science 298:1620–1623 (2002).

Park Y, Mengus G, Bai X, Kageyama Y, Meller VH, et al: Sequence-specific targeting of *Drosophila roX* genes by the MSL dosage compensation complex. Mol Cell 11:977–986 (2003).

Wiegant J, Verwoerd N, Mascheretti S, Bolk M, Tanke HJ, Raap AK: An evaluation of a new series of fluorescent dUTPs for fluorescence in situ hybridization. J Histochem Cytochem 44:525–529 (1996).